

Accurate ground-state energies of Wigner crystals from a simple real-space approach

Estefania Alves,¹ Gian Luigi Bendazzoli,² Stefano Evangelisti,^{3,*} and J. Arjan Berger^{3,4,†}

¹*CEMES/CNRS, 29 rue J. Marvig, 31055 Toulouse, France*

²*Università di Bologna, Bologna, Italy*

³*Laboratoire de Chimie et Physique Quantiques, CNRS, Université de Toulouse, UPS, 118 route de Narbonne, F-31062 Toulouse, France*

⁴*European Theoretical Spectroscopy Facility (ETSF)*

(Dated: March 3, 2021)

We propose a simple and efficient real-space approach for the calculation of the ground-state energies of Wigner crystals in 1, 2, and 3 dimensions. To be precise, we calculate the first two terms in the asymptotic expansion of the total energy per electron which correspond to the classical and zero-point energies of the Wigner crystals. Our approach employs Clifford periodic boundary conditions to simulate the infinite electron gas and a renormalized distance to evaluate the Coulomb potential. This allows us to calculate the energies unambiguously and with a higher precision than those reported in the literature. Our results are in agreement with the literature values with the exception of the zero-point energy of the 2-dimensional Wigner crystal for which we find a significant difference. Although we focus on the ground state, i.e., the triangular lattice and the body-centered cubic lattice, in two and three dimensions, respectively, we also report the classical energies of several other common lattice structures.

I. INTRODUCTION

The uniform electron gas (UEG)^{1,2}, otherwise known as jellium, has proven to be a very useful model for the understanding of electron interactions. In particular in the solid state the UEG can be used to study a variety of phenomena, such as plasmon oscillations³, electron screening⁴, the quantum Hall effect⁵ and Wigner localization^{6–10}. Moreover, by combining the UEG with density-functional theory (DFT) predictive calculations can be performed on both solids and molecules. Thanks to quantum Monte Carlo calculations¹¹ the correlation contribution to the ground-state energy of the UEG as a function of the density is accurately known. This data has been used to approximate the unknown exchange-correlation energy of DFT.^{12–14}

Almost a century ago, it was predicted by Wigner⁶ that in the limit of an infinitely dilute UEG the electrons crystallize at fixed positions in space, thus forming a crystal lattice. Wigner crystals have later been experimentally realized in 1D and 2D and have shown to exhibit interesting properties.^{15,16} However, numerical calculations were required to determine the ground-state crystal structures in both 2D and 3D. By comparing the energies of several Bravais lattices it was concluded that in 2D the electrons crystallize in the triangular structure¹⁷ while in 3D they crystallize in the body-centered cubic structure.^{6,18–20}

The energy per electron of a Wigner crystal E_{WC} can be written as an asymptotic expansion in powers of $r_s^{-\frac{1}{2}}$:²¹

$$E_{WC} \sim \frac{\eta_0}{r_s} + \frac{\eta_1}{r_s^{3/2}} + \frac{\eta_2}{r_s^2} + \frac{\eta_3}{r_s^{5/2}} + \dots \quad (1)$$

where r_s is the Wigner-Seitz radius. The first term on the right-hand side is the energy corresponding to a classical charge distribution, the second term is a correction

due to the zero-point motion in the harmonic approximation, while η_2, η_3, \dots correspond to anharmonic corrections. In this work we will focus on the calculation of η_0 and η_1 . These parameters have been calculated in the past using reciprocal-space approaches. Here we will show that they can also be calculated within a simple real-space method. We note that Eq. (1) assumes that the electrons are discernable.⁶ However, for large r_s the corresponding error is negligible since the correction falls off exponentially with r_s .

For the 3D Wigner crystal the first accurate calculation of the classical ground-state energy per electron was done by Fuchs.¹⁸ He obtained $\eta_0^{3D} = -0.895\,93$ Ha. This value was later refined to $\eta_0^{3D} = -0.895\,929$ Ha by Hasse and Avilov²⁰. The first estimation of the zero-point energy per electron was done by Wigner who found $\eta_1^{3D} = 2.7$ Ry.²² This result is quite close to those obtained two decades later by Coldwell-Horsfall and Maradudin and by Carr. They found $\eta_1^{3D} = 1.319$ Ha²³ and $\eta_1^{3D} = 1.33$ Ha.²¹, respectively. Using the same approach as Carr but with an improved integration over the Brillouin zone, Nagai and Fukuyama found the most accurate value to date, i.e., $\eta_1^{3D} = 1.328\,62$ Ha.²⁴

Both the classical ground-state energy per electron and the zero-point energy per electron of the 2D Wigner crystal have been calculated by Bonsall and Maradudin¹⁷. They found $\eta_0^{2D} = 1.106\,103$ Ha and $\eta_1^{2D} = 0.795$ Ha. To the best of our knowledge this is the only calculation for η_1^{2D} in the literature. Below we will show that we obtain a value with a much higher precision and which differs significantly from the value of Bonsall and Maradudin.

In 1D the classical ground-state energy per electron diverges because of a non-integrable singularity in the 1D Coulomb potential in the origin. Therefore, we will not consider the calculation of η_0^{1D} . We note, however, that regularization techniques can be used for the Coulomb potential to allow for its calculation.^{25–27}. Instead, η_1^{1D}

TABLE I. Summary of the most accurate literature values (in Ha.) of the coefficients η_0 and η_1 .

	1D	2D	3D
	linear lattice	triangular lattice	bcc lattice
η_0	-	-1.106 103 ¹⁷	-0.895 929 ²⁰
η_1	0.359 933 ²⁵	0.795 ¹⁷	1.328 62 ²⁴

can be calculated without problems and its value has been determined with high accuracy.²⁵⁻²⁷ Its 6-digit approximation is $\eta_1^{1D} = 0.359\,933$ Ha. In table I we summarize the most accurate values for η_0 and η_1 that can be found in the literature.

The goal of this work is two-fold: 1) to present a simple and general real-space approach for the calculation of the coefficients η_0 and η_1 and 2) to give a larger precision of those coefficients, in particular for η_1 , for Wigner crystals in 2D, and 3D. We will use an approach based on Clifford boundary conditions and a renormalized distance²⁸ that we previously have successfully applied to the calculation of Madelung constants.²⁹

The paper is organized as follows. In section II we describe the theoretical details of our real-space approach. In section III we discuss our results for the energies of the Wigner crystals. Finally, in section IV we draw our conclusions. We use Hartree atomic units ($\hbar = e = m_e = a_0 = 1$) throughout this work.

II. THEORY

A. The jellium model

The Hamiltonian of an infinite uniform electron gas with a uniform positive background that ensures the charge neutrality of the system is given by

$$\hat{H}_{jellium} = - \sum_i \frac{\nabla_{\vec{r}_i}^2}{2} + \hat{U}_{ee} + \hat{U}_{bb} + \hat{U}_{eb}, \quad (2)$$

in which the electron-electron, electron-background, and background-background contributions to the Coulomb potential are given by, respectively,

$$\hat{U}_{ee} = \frac{1}{2} \sum_{\substack{i,j \\ i \neq j}} \frac{1}{|\vec{r}_i - \vec{r}_j|}, \quad (3)$$

$$\hat{U}_{eb} = - \sum_i \int d\vec{r} \frac{n}{|\vec{r} - \vec{r}_i|}, \quad (4)$$

$$\hat{U}_{bb} = \frac{1}{2} \int d\vec{r} \int d\vec{r}' \frac{n^2}{|\vec{r} - \vec{r}'|}, \quad (5)$$

where n is the uniform positive background density. The charge neutrality of the system is imposed by assuming

that the constant electron density is equal, but with opposite sign, to the positive background density n . Individually each term in Eq. (2) diverges but their sum is finite, except for the one-dimensional uniform electron gas.

At low density the electrons form a Wigner crystal with the electrons localized at the lattice positions of a crystal. Therefore, we can perform a Taylor expansion of the Coulomb potential around \vec{R} the equilibrium lattice vectors of the electrons in the Wigner crystal.

$$\hat{H}_{jellium} = -\frac{1}{2} \sum_i \nabla_{\vec{r}_i}^2 + \hat{U}_0 + \hat{U}_2 + \dots \quad (6)$$

in which

$$\hat{U}_0 = \frac{1}{2} \sum_{\substack{i,j \\ i \neq j}} \frac{1}{|\vec{R}_i - \vec{R}_j|} - \sum_i \int d\vec{r} \frac{n}{|\vec{r} - \vec{R}_i|} + \hat{U}_{bb} \quad (7)$$

$$\hat{U}_2 = \frac{1}{2} \sum_{ij} \sum_{\alpha\beta} \partial_{i\alpha} \partial_{j\beta} \hat{U}_{ee} \Big|_{r_{i,\alpha}=R_{i,\alpha}, r_{j,\beta}=R_{j,\beta}} \times (r_{i,\alpha} - R_{i,\alpha})(r_{j,\beta} - R_{j,\beta}), \quad (8)$$

where the Greek letters α and β denote Cartesian components. Since the classical energy U_0 is a minimum, the contribution of the first order term in the expansion, \hat{U}_1 , vanishes. Furthermore, only variations in \hat{U}_{ee} contribute to \hat{U}_2 since \hat{U}_{bb} is independent of the electronic coordinates and variations in the electronic position do not change \hat{U}_{be} because of the uniformity of the background. In this work we will consider the first three terms on the right-hand side of Eq. (6). This allows us to calculate the first two coefficients in Eq. (1).

Defining the relative coordinates $\vec{u}_i = \vec{r}_i - \vec{R}_i$ we can rewrite the first three terms of Eq. (6) in the following general form²¹

$$\hat{H} = \hat{U}_0 - \frac{1}{2} \sum_i \nabla_{\vec{u}_i}^2 + \frac{1}{2} \sum_{\substack{i,j \\ i \neq j}} \sum_{\alpha\beta} C_{\alpha\beta}(\vec{R}_i - \vec{R}_j) u_{i,\alpha} u_{j,\beta}, \quad (9)$$

in which the real symmetric matrix \mathbf{C} is defined as

$$C_{\alpha\beta}(\vec{R}_i - \vec{R}_j) = \partial_{i\alpha} \partial_{j\beta} \frac{1}{|\vec{u}_i - \vec{u}_j + \vec{R}_i - \vec{R}_j|} \Big|_{\vec{u}=0} \quad (10)$$

where the derivatives are now with respect to \vec{u} .

Thanks to the translational invariance of the system we can use the following Fourier transformation

$$\vec{u}_j = \frac{1}{\sqrt{\mathcal{N}}} \sum_k e^{i\vec{G}_k \cdot \vec{R}_j} \vec{v}_k \quad (11)$$

$$\vec{v}_k = \frac{1}{\sqrt{\mathcal{N}}} \sum_j e^{-i\vec{G}_k \cdot \vec{R}_j} \vec{u}_j, \quad (12)$$

where \mathcal{N} is a normalisation constant and the \vec{G}_k can be

interpreted as reciprocal lattice vectors, to rewrite Eq. (9) as

$$\hat{H} = \hat{U}_0 + \sum_k \left[-\frac{1}{2} \nabla_{\vec{v}_k}^2 + \frac{1}{2} \sum_{\alpha\beta} \tilde{C}_{\alpha\beta}(\vec{G}_k) v_{k,\alpha} v_{k,\beta}^* \right] \quad (13)$$

with

$$\tilde{C}_{\alpha\beta}(\vec{G}_k) = \sum_i C_{\alpha\beta}(\vec{R}_i) e^{i\vec{G}_k \cdot \vec{R}_i} \quad (14)$$

a real symmetric $d \times d$ matrix with $d = 1, 2, 3$ the dimensionality of the lattice. Finally, using the eigenvectors of $C(\vec{G}_k)$ we can perform an orthonormal transformation to arrive at

$$\hat{H} = \hat{U}_0 + \sum_k \sum_{\alpha} \left[-\frac{1}{2} \partial_{k,\alpha}^2 + \frac{1}{2} \omega_{k,\alpha}^2 q_{k,\alpha}^2 \right], \quad (15)$$

where $\omega_{k,\alpha}^2$ are the eigenvalues of $\tilde{C}(\vec{G}_k)$ and \vec{q}_k are normal modes. The expression inside the square brackets in the above equation is the Hamiltonian of a quantum harmonic oscillator in one dimension for which the eigenenergies are known. Therefore, the total ground-state energy per electron of the Wigner crystal can be written as

$$E_{WC} \sim \frac{\eta_0}{r_s} + \frac{\eta_1}{r_s^{3/2}} + \dots, \quad (16)$$

with

$$\frac{\eta_0}{r_s} = \frac{U_0}{N} \quad (17)$$

$$\frac{\eta_1}{r_s^{3/2}} = \frac{1}{2N} \sum_k \sum_{\alpha} \omega_{k,\alpha}. \quad (18)$$

The jellium problem pertains to a system with an infinite number of electrons in an infinite volume at constant density. In practical calculations we can of course only deal with a finite number of electrons in a finite volume. However, we would like to preserve the translational symmetry of the jellium model. Therefore, we impose periodic boundary conditions with respect to a finite supercell. Unfortunately, the long-range Coulomb potential is not periodic and it does not vanish at the borders of any, even very large, finite supercell. Therefore, as explained in the next section, we impose Clifford boundary conditions with a renormalized distance.

B. Clifford boundary conditions

We will use Clifford boundary conditions which means that we define a supercell that has the topology of a Clifford torus, i.e., a finite, flat and borderless manifold. A Clifford supercell is linked to a Euclidean supercell defined in \mathbb{R}^d . The Clifford supercell is then obtained by joining opposite sides of the Euclidean supercell *without*

deformation. This can be achieved by defining the Clifford supercell in the embedding space \mathbb{C}^2 (alternatively, it can also be achieved in \mathbb{R}^{2D}).

Let us consider a general orthorhombic lattice in d dimensions and define \vec{a}_α to be the orthogonal generating vectors of a unit cell in \mathbb{R}^d . Then a general vector \vec{v} inside the unit cell can be written as

$$\vec{v} = \sum_{\alpha} x_{\alpha} \vec{a}_{\alpha}, \quad (19)$$

where $0 \leq x_{\alpha} < 1$. We define a Euclidean supercell (ESC) as the right parallelepiped in \mathbb{R}^d generated by the vectors \vec{A}_α given by

$$\vec{A}_\alpha = K_\alpha \vec{a}_\alpha. \quad (20)$$

where K_α are positive integers. The ESC thus contains $\prod_{\alpha} K_\alpha$ copies of the unit cell. A general vector \vec{r}^{ESC} in the ESC can thus be written as

$$\vec{r}^{ESC} = \vec{v} + \sum_{\alpha} k_{\alpha} \vec{a}_{\alpha} = \sum_{\alpha} x_{\alpha} \vec{a}_{\alpha} \quad (21)$$

with $r_{\alpha} = x_{\alpha} + k_{\alpha}$ and $0 \leq k_{\alpha} \leq K_{\alpha} - 1$.

We now define the Clifford supercell (CSC) as the Clifford torus in which the opposite borders (either points, edges, or faces, depending on d) of the corresponding ESC are connected without deformation. A general vector \vec{r}^{CSC} in the CSC should respect the translational symmetry of the Clifford torus. This can be achieved by writing \vec{r}^{CSC} according to

$$\vec{r}^{CSC} = \sum_{\alpha} \frac{K_{\alpha}}{2\pi i} \left[e^{i2\pi r_{\alpha}/K_{\alpha}} - 1 \right] \vec{a}_{\alpha}. \quad (22)$$

We note that the above expression is the classical equivalent of the PBC position operator proposed by some of us in a quantum context.²⁸ The above definition satisfies a number of important constraints. In particular, it satisfies the translational symmetry, it reduces to the standard position operator in the appropriate limit and the corresponding definition of the distance is real and gauge invariant (see Eq. (23) below).²⁸

In order to evaluate Coulomb potentials we have to define the distance between two points in the CSC. We note that a possibility would be to define the distance as the smallest difference between two points *on* the Clifford torus. However, such a distance would have discontinuous derivatives in those points of the CSC that correspond to the midpoints of the edges of the corresponding ESC. This would yield discontinuous forces in these points, which is unphysical. Therefore, we choose the distance to be the Euclidean norm in \mathbb{C}^d because it is both uniquely defined and yields continuous derivatives. In other words, the distance is defined in the embedding space of the Clifford torus. This distance

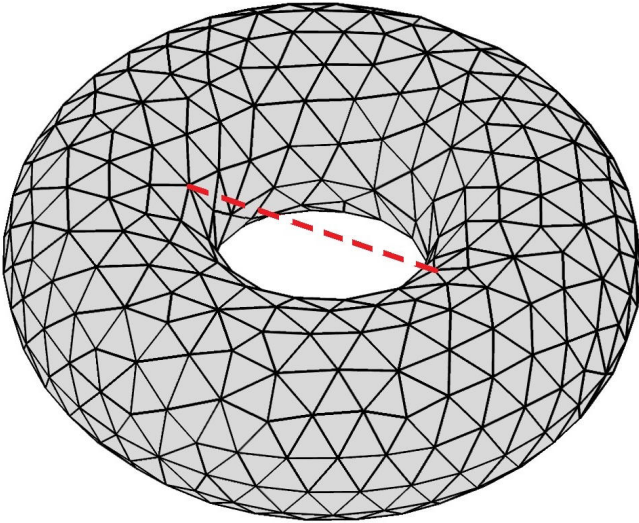


FIG. 1. Pictorial illustration of a Clifford supercell for the triangular lattice of the 2-dimensional Wigner crystal. The equilibrium positions of the electrons are located at the vertices. The dashed red line represents the renormalized distance between two electrons used in the Coulomb potential. It is the shortest distance in the embedding space of the Clifford torus. We note that a true Clifford torus has a flat surface which is impossible to represent graphically.

$r_{ij}^{CSC} = |\vec{r}_i^{CSC} - \vec{r}_j^{CSC}|$ is given by

$$r_{ij}^{CSC} = \sqrt{\sum_{\alpha} \frac{L_{\alpha}^2}{\pi^2} \sin^2 \left(\frac{\pi}{L_{\alpha}} [r_{i\alpha} - r_{j\alpha}] \right)}, \quad (23)$$

where we used that $\vec{a}_{\alpha} \cdot \vec{a}_{\beta} = 0$ for $\alpha \neq \beta$ and $L_{\alpha} = K_{\alpha} |\vec{a}_{\alpha}|$ with L_{α} the length of an edge of the ESC. We will evaluate the Coulomb potentials in Eqs. (7) and (8) using the above renormalized distance. In Fig. 1 we show an illustration of a CSC for a 2-dimensional Wigner crystal and the renormalized distance between the electrons.

C. The 3D Wigner crystal

With the renormalized distance the background-background contribution in the 3D CSC is given by

$$\hat{U}_{bb}^{CSC} = \frac{N^2}{2V} \int_V \frac{dx dy dz}{\sqrt{\frac{L_x^2}{\pi^2} \sin^2[\frac{\pi x}{L_x}] + \frac{L_y^2}{\pi^2} \sin^2[\frac{\pi y}{L_y}] + \frac{L_z^2}{\pi^2} \sin^2[\frac{\pi z}{L_z}]}} \quad (24)$$

$$\hat{U}_{0,ee}^{CSC} = \frac{1}{2} \sum_{\substack{i,j \\ i \neq j}} \frac{1}{\sqrt{\frac{L_x^2}{\pi^2} \sin^2[\frac{\pi}{L_x} (x_i - x_j)] + \frac{L_y^2}{\pi^2} \sin^2[\frac{\pi}{L_y} (y_i - y_j)] + \frac{L_z^2}{\pi^2} \sin^2[\frac{\pi}{L_z} (z_i - z_j)]}} \quad (29)$$

This is the only contribution that depends on the details

where, thanks to the periodicity of the CSC, we could reduce the two volume integrals to only one and we used that $n = N/V$, which ensures the charge neutrality of the 3D CSC supercell, with $V = L_x L_y L_z$ the volume of the supercell. With the changes of variable $\theta_x = \frac{\pi x}{L}$, $\theta_y = \frac{\pi y}{L}$, and $\theta_z = \frac{\pi z}{L}$ the above expression can be rewritten according to

$$\hat{U}_{bb}^{CSC} = \frac{N^2}{2\pi^2} \int_0^{\pi} \int_0^{\pi} \int_0^{\pi} \frac{d\theta_x d\theta_y d\theta_z}{\sqrt{L_x^2 \sin^2 \theta_x + L_y^2 \sin^2 \theta_y + L_z^2 \sin^2 \theta_z}}. \quad (25)$$

The triple integral in the above equation can be readily calculated. For example, in the case of a cubic supercell, i.e., $L = L_x = L_y = L_z$, we obtain the following result

$$\hat{U}_{bb}^{CSC} = \frac{N^2 \gamma_c}{L} \quad (L = L_x = L_y = L_z) \quad (26)$$

with $\gamma_c = 1.4305055275$.

Thanks to the periodicity and uniformity of the positive background, each electron contributes exactly the same amount to the summation in the expression of the electron-background contribution in the CSC. Therefore, without loss of generality, we can choose to consider explicitly only the contribution of an electron located at the origin and multiply with N . We can thus write the electron-background contribution according to

$$\hat{U}_{eb}^{CSC} = -\frac{N^2}{V} \int_V \frac{dx dy dz}{\sqrt{\frac{L_x^2}{\pi^2} \sin^2[\frac{\pi x}{L_x}] + \frac{L_y^2}{\pi^2} \sin^2[\frac{\pi y}{L_y}] + \frac{L_z^2}{\pi^2} \sin^2[\frac{\pi z}{L_z}]}}. \quad (27)$$

where we once more used $n = N/V$. We note that in the special case $L = L_x = L_y = L_z$ the integral in the above equation can be made independent of L in a similar way as was done for \hat{U}_{bb} . By comparing Eqs. (24) and (27) we find the following identity between \hat{U}_{bb} and \hat{U}_{eb} in the CSC,

$$\hat{U}_{eb}^{CSC} = -2\hat{U}_{bb}^{CSC}. \quad (28)$$

Finally, the classical electron-electron contribution $\hat{U}_{0,ee}$ in the CSC is given by

of the lattice structure, i.e., the equilibrium positions of

the electrons.

In the following we will focus on the body-centered cubic (bcc) lattice since it yields the ground-state energy of a 3D Wigner crystal. A similar strategy as described below can be used for other lattices. For the bcc structure it is convenient to use a cubic supercell, i.e., $L = L_x = L_y = L_z$ and to define the equilibrium positions of the electrons according to $\vec{R}_i = (\pi/3)^{1/3} r_s \vec{n}_i$ with \vec{n}_i a vector of three integers, all even or all odd.²¹ Therefore, $L = (\pi/3)^{1/3} (2N_s) r_s$ with N_s the number of electrons per side. The total classical bcc energy $U_0 = U_{0,ee}^{CSC} - U_{bb}^{CSC}$ per electron can thus be written as

$$\frac{U_0}{N} = \frac{\left(\frac{3}{\pi}\right)^{1/3}}{2N_s r_s} \left[\frac{\pi}{2} \sum_{i=1}^N \left(\sum_{\alpha} \sin^2 \left[\frac{\pi n_{i\alpha}}{2N_s} \right] \right)^{-1/2} - \gamma_c N \right]. \quad (30)$$

Since $U_0/N = \eta_0^{bcc}/r_s$ we can easily obtain η_0^{bcc} from the above expression.

For the bcc lattice the \mathbf{C} matrix defined in Eq. (10) is given by

$$C_{\alpha\beta}^{N_s}(\vec{0}) = -\frac{3\pi^2}{8N_s^3} \frac{\delta_{\alpha\beta}}{r_s^3} \sum_{\vec{n}_i \neq \vec{0}} \left[\frac{\cos\left[\frac{\pi n_{i\alpha}}{N_s}\right]}{(\sum_{\alpha'} \sin^2[\pi n_{i\alpha'}/(2N_s)])^{3/2}} - \frac{3/4 \sin^2\left[\frac{\pi n_{i\alpha}}{N_s}\right]}{(\sum_{\alpha'} \sin^2[\pi n_{i\alpha'}/(2N_s)])^{5/2}} \right] \quad (31)$$

$$C_{\alpha\beta}^{N_s}(\vec{n}_i) = \frac{3\pi^2}{8N_s^3} \frac{1}{r_s^3} \left[\frac{\delta_{\alpha\beta} \cos\left[\frac{\pi n_{i\alpha}}{N_s}\right]}{\sum_{\alpha'} (\sin^2[\pi n_{i\alpha'}/(2N_s)])^{3/2}} - \frac{3/4 \sin\left[\frac{\pi n_{i\alpha}}{N_s}\right] \sin\left[\frac{\pi n_{i\beta}}{N_s}\right]}{\sum_{\alpha'} (\sin^2[\pi n_{i\alpha'}/(2N_s)])^{5/2}} \right] \quad (\vec{n}_i \neq \vec{0}). \quad (32)$$

where the summation in Eq. (31) is over all $\vec{n}_i \neq \vec{0}$ inside the CSC. We note that in the limit $N_s \rightarrow \infty$ we have the following identity

$$\lim_{N_s \rightarrow \infty} C_{\alpha\alpha}^{N_s}(\vec{0}) = \frac{1}{8r_s^3}. \quad (33)$$

The matrix \tilde{C} given in Eq. (14) can be rewritten as

$$\tilde{C}^{N_s}(\vec{n}_k) = \sum_{\vec{n}_i} C^{N_s}(\vec{n}_i) \cos\left(\frac{\pi \vec{n}_k \cdot \vec{n}_i}{N_s}\right) \quad (34)$$

where we used that $\vec{G}_k = 2\pi \vec{n}_k / (2N_s)$. To obtain η_1^{bcc} it suffices to diagonalize $\tilde{C}^{N_s}(\vec{n}_k) \forall k$, take the square root of the eigenvalues and add them up according to Eq. (18).

D. The 2D Wigner crystal

The derivation of the various terms of the Coulomb potential in 2D for the CSC are analogous to those of the 3D

Wigner crystal discussed in the previous subsection. The background-background and electron-background contributions in the CSC are given by

$$\hat{U}_{bb}^{CSC} = -\frac{\hat{U}_{eb}}{2} = \frac{N^2}{2\pi} \int_0^\pi \int_0^\pi \frac{d\theta_x d\theta_y}{\sqrt{L_x^2 \sin^2 \theta_x + L_y^2 \sin^2 \theta_y}} \quad (35)$$

where we used that in 2D $n = N/(L_x L_y)$. We note that in the special case $L = L_x = L_y$ we obtain the following analytical expression

$$\hat{U}_{bb}^{CSC} = -\frac{\hat{U}_{eb}}{2} = \frac{N^2}{2\sqrt{\pi}L} G_{3,3}^{2,2} \left(\begin{matrix} 1, 1, 1 \\ 1/2, 1/2, 1/2 \end{matrix} \middle| 1 \right) \quad (36)$$

where G is the Meijer G function. The classical electron-electron contribution in the 2D CSC is given by

$$\hat{U}_{0,ee}^{CSC} = \frac{1}{2} \sum_{\substack{i,j \\ i \neq j}} \frac{1}{\sqrt{\frac{L_x^2}{\pi^2} \sin^2\left[\frac{\pi}{L_x}(x_i - x_j)\right] + \frac{L_y^2}{\pi^2} \sin^2\left[\frac{\pi}{L_y}(y_i - y_j)\right]}} \quad (37)$$

In the following we will focus on the triangular lattice since it yields the ground-state energy of a 2D Wigner crystal. For the triangular lattice it is convenient to use a rectangular supercell and to define the equilibrium positions of the electrons according to $\vec{R}_i = r_s \sqrt{\pi/(2\sqrt{3})} (n_x, n_y \sqrt{3})^T$ with n_x and n_y two integers, both even or both odd. Therefore, $L_x = 2r_s \sqrt{\pi/(2\sqrt{3})} N_s$ and $L_y = r_s \sqrt{\pi/2\sqrt{3}} N_s$. The total classical energy $U_0 = U_{0,ee}^{CSC} - U_{bb}^{CSC}$ per electron of the triangular lattice can thus be written as

$$\frac{U_0}{N} = \frac{1}{N_s r_s} \left[\frac{\sqrt{\pi}}{2\sqrt{2}} \sum_{i=1}^N \frac{3^{1/4}}{\sqrt{f(\vec{n}_i)}} - \gamma_t N \right], \quad (38)$$

where $\gamma_t = 0.7839363355$ and

$$f(\vec{n}_i) = \sin^2 \left[\frac{\pi n_{ix}}{2N_s} \right] + 3 \sin^2 \left[\frac{\pi n_{iy}}{2N_s} \right]. \quad (39)$$

For the triangular lattice the \mathbf{C} matrix defined in Eq. (10) is given by

$$C_{\alpha\beta}^{N_s}(\vec{0}) = -\left(\frac{\pi\sqrt{3}}{2N_s^2}\right)^{3/2} \frac{\delta_{\alpha\beta}}{r_s^3} \sum_{\vec{n}_i \neq \vec{0}} \left[\frac{\cos\left[\frac{\pi n_{i\alpha}}{N_s}\right]}{f(\vec{n}_i)^{3/2}} - \frac{3(\sqrt{3})^{\delta_{\alpha y}} (\sqrt{3})^{\delta_{\beta y}} \sin^2\left[\frac{\pi n_{i\alpha}}{N_s}\right]}{f(\vec{n}_i)^{5/2}} \right] \quad (40)$$

$$C_{\alpha\beta}^{N_s}(\vec{n}_i) = \left(\frac{\pi\sqrt{3}}{2N_s^2}\right)^{3/2} \frac{1}{r_s^3} \left[\frac{\delta_{\alpha\beta} \cos\left[\frac{\pi n_{i\alpha}}{N_s}\right]}{f(\vec{n}_i)^{3/2}} - \frac{3(\sqrt{3})^{\delta_{\alpha y}} (\sqrt{3})^{\delta_{\beta y}} \sin\left[\frac{\pi n_{i\alpha}}{N_s}\right] \sin\left[\frac{\pi n_{i\beta}}{N_s}\right]}{f(\vec{n}_i)^{5/2}} \right] \quad (\vec{n}_i \neq \vec{0}), \quad (41)$$

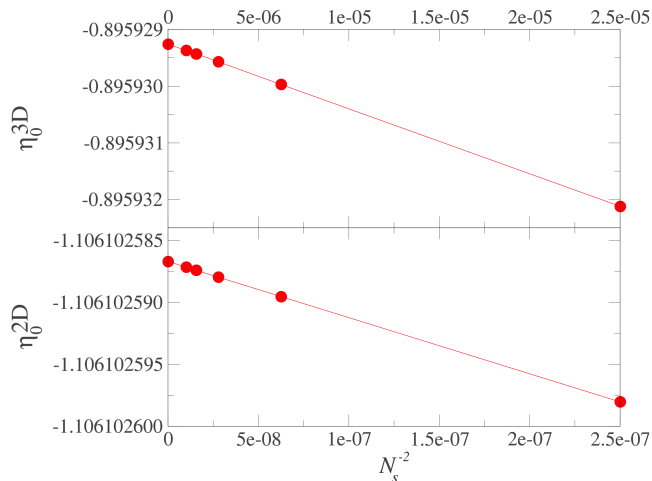


FIG. 2. The coefficient η_0 as a function of N_s^{-2} for the 3D bcc lattice and the 2D triangular lattice. The dots at $N_s^{-2} = 0$ indicate the extrapolated values obtained according to Eq. (45).

where the summation in Eq. (40) is over all $\vec{n}_i \neq \vec{0}$ inside the CSC. A similar procedure as described for the 3D bcc lattice in the previous subsection then leads to η_1^{2D} .

E. The 1D Wigner Crystal

As mentioned in the Introduction, in 1D the classical ground-state energy per electron diverges because of a non-integrable singularity in the 1D Coulomb potential. Therefore we will focus here on the calculation of η_1 . In 1D the C matrix defined in Eq. (10) is just a number that is given by

$$C^N(0) = \frac{\pi^3}{8N^3} \frac{1}{r_s^3} \sum_{n=1}^{N-1} \frac{1 + \cos^2[\pi n/N]}{|\sin[\pi n/N]|^3} \quad (42)$$

$$C^N(n) = -\frac{\pi^3}{8N^3} \frac{1}{r_s^3} \frac{1 + \cos^2[\pi n/N]}{|\sin[\pi n/N]|^3} \quad (n \neq 0). \quad (43)$$

We note that in the limit $N \rightarrow \infty$ we have the following identity

$$\lim_{N \rightarrow \infty} C^N(0) = \frac{\zeta(3)}{4r_s^3} \quad (44)$$

in terms of the Riemann ζ function.

III. RESULTS

We summarize here the results obtained for η_0 and η_1 for various lattices in the limit of the infinite systems. To estimate the coefficients η_0 and η_1 for the infinite CSC we extrapolate the coefficients of finite-size CSC with the

TABLE II. Ground-state energies for the square and triangular 2D crystal structures (in Ha/ r_s)

Lattice	η_0^{2D}	
	this work	literature ¹⁷
square	-1.100 244 420	-1.100 244
triangle	-1.106 102 587	-1.106 103

TABLE III. Ground-state energies for several 3D crystal structures (in Ha/ r_s)

Lattice	η_0^{3D}	
	this work	literature ²⁰
simple cubic	-0.880 059 442	-0.880 059
body-centered cubic	-0.895 929 255	-0.895 929
face-centered cubic	-0.895 873 614	-0.895 874
hexagonal close packed	-0.895 838 120	-0.895 838

following power function,

$$\eta(N_s) = \eta_\infty + AN_s^{-2}, \quad (45)$$

where A and η_∞ are the fit coefficients. This power function has also proven to work well for the extrapolation of Madelung constants²⁹.

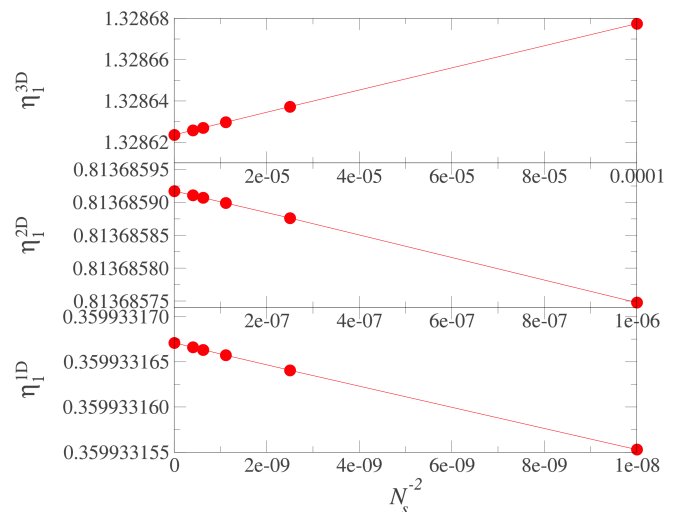


FIG. 3. The coefficient η_1 as a function of N_s^{-2} for the 3D bcc lattice, the 2D triangular lattice, and the 1D linear lattice. The dots at $N_s^{-2} = 0$ indicate the extrapolated values obtained according to Eq. (45).

TABLE IV. η_1 for Wigner crystals in 1D, 2D, and 3D (in Ha/r_s)

Lattice	η_1	
	this work	literature
1D (linear)	0.359 933	0.359 933 ²⁵
2D (triangular)	0.813 686	0.795 ¹⁷
3D (body-centered cubic)	1.328 624	1.328 62 ²¹

TABLE V. Summary of the the coefficients η_0 and η_1 obtained in this work.

	1D	2D	3D
	linear lattice	triangular lattice	bcc lattice
η_0	-	-1.106 103	-0.895 929
η_1	0.359 933	0.813 686	1.328 624

A. The classical energy, η_0

In Fig. 2 we report η_0^{3D} and η_0^{2D} as a function of N_s^{-2} , for the bcc and triangular lattice respectively.

We can use the same strategy to find the ground-state energy for any crystal structure. For the sake of completeness we report in Tables II and III the ground-state energies of the most common crystal structures in 2D and 3D, respectively. As expected we find that in 2D the triangular lattice is lower in energy than the square lattice, while in 3D, it is the bcc lattice that has the lowest energy, although the difference with the fcc and hcp lattices

are small. Our results are in perfect agreement with the literature values while with our approach we can easily obtain several more digits.

B. The harmonic correction, η_1

In Fig. 3 we report η_1 as a function of N_s^{-2} for 1D, 2D, and 3D. Again the results are close to linear and we can extrapolate to the infinite-size CSC with the power function of Eq. (45). We report the extrapolated values in Table IV. We see that for the 1D and 3D Wigner crystals our results are in agreement with the most accurate values found in the literature. Instead, for the triangular 2D Wigner crystal our result is significantly different from the literature value.

IV. CONCLUSIONS

We have presented a simple real-space approach for the calculation of the ground-state energy of Wigner crystals in one, two and three dimensions. Our approach yields values with high precision for the first two terms in the asymptotic expansion of the energy per electron of Wigner crystals. Our results are in agreement with the values found in the literature with the exception of the zero-point energy of the 2D triangular Wigner crystal for which we find a significantly larger value than the one found in the literature. We summarized our results in Table V.

* stefano.evangelisti@irsamc.ups-tlse.fr

† arjan.berger@irsamc.ups-tlse.fr

¹ G. F. Giuliani and G. Vignale, *Quantum theory of the electron liquid* (Cambridge University Press).

² Pierre-François Loos and Peter M. W. Gill, “The uniform electron gas,” *WIREs Computational Molecular Science* **6**, 410–429 (2016).

³ Lewi Tonks and Irving Langmuir, “Oscillations in ionized gases,” *Phys. Rev.* **33**, 195–210 (1929).

⁴ J Lindhard, “On the properties of a gas of charged particles,” *Danske Matematisk-fysiske Meddeleiser* **28**, 1–54 (1954).

⁵ K. v. Klitzing, G. Dorda, and M. Pepper, “New method for high-accuracy determination of the fine-structure constant based on quantized hall resistance,” *Phys. Rev. Lett.* **45**, 494–497 (1980).

⁶ E. Wigner, “On the interaction of electrons in metals,” *Phys. Rev.* **46**, 1002–1011 (1934).

⁷ K Jauregui, W Häusler, and B Kramer, “Wigner molecules in nanostructures,” *Europhysics Letters (EPL)* **24**, 581–587 (1993).

⁸ Alejandro Diaz-Marquez, Stefano Battaglia, Gian Luigi Bendazzoli, Stefano Evangelisti, Thierry Leininger, and

J. A. Berger, “Signatures of wigner localization in one-dimensional systems,” *J. Chem. Phys.* **148**, 124103 (2018).

⁹ Miguel Escobar Azor, Léa Brooke, Stefano Evangelisti, Thierry Leininger, Pierre-François Loos, Nicolas Suaud, and J A Berger, “A wigner molecule at extremely low densities: a numerically exact study,” *SciPost Phys. Core* **1**, 001 (2019).

¹⁰ Niccolo Traverso Ziani, Fabio Cavaliere, Karina Guerrero Becerra, and Maura Sasseti, “A short review of one-dimensional wigner crystallization,” *Crystals* **11** (2021).

¹¹ D. M. Ceperley and B. J. Alder, “Ground state of the electron gas by a stochastic method,” *Phys. Rev. Lett.* **45**, 566–569 (1980).

¹² S. H. Vosko, L. Wilk, and M. Nusair, “Accurate spin-dependent electron liquid correlation energies for local spin density calculations: a critical analysis,” *Canadian Journal of Physics* **58**, 1200–1211 (1980).

¹³ J. P. Perdew and Alex Zunger, “Self-interaction correction to density-functional approximations for many-electron systems,” *Phys. Rev. B* **23**, 5048–5079 (1981).

¹⁴ John P. Perdew and Yue Wang, “Accurate and simple analytic representation of the electron-gas correlation energy,” *Phys. Rev. B* **45**, 13244–13249 (1992).

- ¹⁵ I. Shapir, A. Hamo, S. Pecker, C. P. Moca, Ö. Legeza, G. Zarand, and S. Ilani, “Imaging the electronic wigner crystal in one dimension,” *Science* **364**, 870–875 (2019).
- ¹⁶ C. C. Grimes and G. Adams, “Evidence for a liquid-to-crystal phase transition in a classical, two-dimensional sheet of electrons,” *Phys. Rev. Lett.* **42**, 795–798 (1979).
- ¹⁷ Lynn Bonsall and A. A. Maradudin, “Some static and dynamical properties of a two-dimensional wigner crystal,” *Phys. Rev. B* **15**, 1959–1973 (1977).
- ¹⁸ K. Fuchs and Ralph Howard Fowler, “A quantum mechanical investigation of the cohesive forces of metallic copper,” *Proceedings of the Royal Society of London. Series A - Mathematical and Physical Sciences* **151**, 585–602 (1935).
- ¹⁹ C A Sholl, “The calculation of electrostatic energies of metals by plane-wise summation,” *Proceedings of the Physical Society* **92**, 434–445 (1967).
- ²⁰ R. W. Hasse and V. V. Avilov, “Structure and madelung energy of spherical coulomb crystals,” *Phys. Rev. A* **44**, 4506–4515 (1991).
- ²¹ W. J. Carr, “Energy, specific heat, and magnetic properties of the low-density electron gas,” *Phys. Rev.* **122**, 1437–1446 (1961).
- ²² E. Wigner, “Effects of the electron interaction on the energy levels of electrons in metals,” *Trans. Faraday Soc.* **34**, 678–685 (1938).
- ²³ Rosemary A. Coldwell-Horsfall and Alexei A. Maradudin, “Zero-point energy of an electron lattice,” *J. Math. Phys.* **1**, 395–404 (1960).
- ²⁴ Tatsuzo Nagai and Hidetoshi Fukuyama, “Ground state of a wigner crystal in a magnetic field i. cubic structure,” *Journal of the Physical Society of Japan* **51**, 3431–3442 (1982).
- ²⁵ Michael M. Fogler, “Ground-state energy of the electron liquid in ultrathin wires,” *Phys. Rev. Lett.* **94**, 056405 (2005).
- ²⁶ Pierre-François Loos and Peter M. W. Gill, “Uniform electron gases. i. electrons on a ring,” *J. Chem. Phys.* **138**, 164124 (2013).
- ²⁷ Pierre-François Loos, “Generalized local-density approximation and one-dimensional finite uniform electron gases,” *Phys. Rev. A* **89**, 052523 (2014).
- ²⁸ Emília Valença Ferreira de Aragão, Diego Moreno, Stefano Battaglia, Gian Luigi Bendazzoli, Stefano Evangelisti, Thierry Leininger, Nicolas Suaud, and J. A. Berger, “A simple position operator for periodic systems,” *Phys. Rev. B* **99**, 205144 (2019).
- ²⁹ Nicolas Tavernier, Gian Luigi Bendazzoli, Véronique Brumas, Stefano Evangelisti, and J. A. Berger, “Clifford boundary conditions: A simple direct-sum evaluation of madelung constants,” *The Journal of Physical Chemistry Letters* **11**, 7090–7095 (2020).